BIOCHEMISTRY
including biophysical chemistry & molecular biology

Article

pubs.acs.org/biochemistry

# Correlation of Heme Binding Affinity and Enzyme Kinetics of Dehaloperoxidase

Peter Le, Jing Zhao, and Stefan Franzen*

Department of Chemistry, North Carolina State University, Raleigh, North Carolina 27695, United States

Supporting Information

**ABSTRACT:** Chemical and thermal denaturation of dehaloperoxidase-hemoglobin (DHP) was investigated to test the relative stability of isoforms DHP A and DHP B and the H55V mutant of DHP A with respect to heme loss. In thermal denaturation experiments, heme loss was observed at temperatures of 54, 46, and 61 °C in DHP A, DHP B, and H55V, respectively. Guanidinium hydrochloride (GdnHCl)- and urea-induced denaturation was observed at respective concentrations of 1.15 ± 0.01 M DHP A and 1.09 ± 0.02 M DHP B, and 5.19 ± 0.05 M DHP A and 4.12 ± 0.14 M DHP B, respectively. The binding affinity of heme appears to be significantly smaller in both isoforms of DHP than in myoglobins. This observation was corroborated by heme transfer experiments, in which heme was observed to transfer for DHP A and B to horse skeletal muscle myoglobin (HSMb). GdnHCl-induced denaturation suggests a threshold of 1 mM for stabilization by binding of the inhibitor 4-bromophenol (4-BP). Concentrations of 4-BP greater than 1 mM caused destabilization. Urea-induced denaturation showed only destabilizing effects from phenolic ligand binding. Heme transfer experiments from DHP to HSMb further support the hypothesis that the binding of halophenols to DHP facilitates the removal of the heme. Thermal denaturation assessed via UV−visible spectroscopy and that assessed by differential scanning calorimetry (DSC) are both in agreement with chemical denaturation experiments and show that the denaturing abilities of the halophenols improve with the size of the para halogen atom in 4-XP, where X = iodo, bromo, chloro, or fluoro (4-IP > 4-BP > 4-CP > 4-FP), and the number of halo substituents as in 2,4,6-tribromophenol (2,4,6-TBP > 4-BP). DHP B, which differs in five amino acids, is less stable than DHP A with $\Delta H_{cal}$ and $T_m$ values of 165.1 kJ/mol and 47.5 °C compared to values of 183.3 kJ/mol and 50.4 °C for DHP B and DHP A, respectively. Kinetic studies verified that DHP B has a catalytic efficiency ($k_{cat}/K_m$) ∼5−6 times greater than that of DHP A but showed an increased level of substrate inhibition in DHP B for both 2,4,6-TCP and 2,4,6-TBP. An inverse correlation between protein stability with respect to heme loss and catalytic efficiency is suggested on the basis of the fact that the heme in DHP B has a stability lower than that of DHP A but a catalytic efficiency higher than that of DHP A.

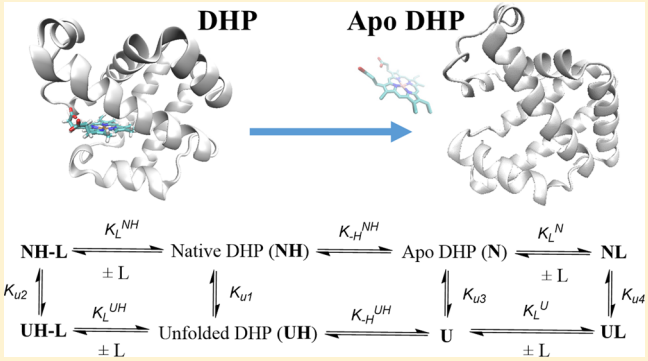


Dehaloperoxidase-hemoglobin (DHP) is a multifunctional enzyme first isolated from the marine worm *Amphitrite ornata*. DHP is capable of oxygen transport in its ferrous state ($Fe^{2+}$) and oxidization of 2,4,6-trihalogenated phenols (2,4,6-TXP) into 2,6-dihalogented quinones (2,6-DXQ) in the presence of $H_2O_2$ in both the ferric ($Fe^{3+}$) and ferrous states.[1,2] Because of its unique role in aquatic ecosystems,[3] DHP is a potential bioremediation enzyme capable of oxidizing several toxic aromatic compounds. DHP was initially identified as a hemoglobin.[4] Later, DHP was discovered to have a peroxidase function.[1] DHP has also recently been shown to have additional capabilities, including oxidase and peroxygenase activities, which leads to the recognition of DHP as a multifunctional protein, able to perform at least four enzymatic functions at a single catalytic active site.[1,2,5−8] This multifunctional enzyme has many characteristics that separate it from both globins (hemoglobin and myoglobin) and peroxidases. DHP contains at least two separate substrate-binding sites and one inhibitor-binding site. Both substrate and inhibitor have internal binding sites observed by X-ray crystallography, NMR, and resonance Raman spectroscopy.[9−16] The presence of one external binding can be inferred from flow-EPR spectroscopy and vibrational Stark effect spectroscopy.[17,18] When a 2,4,6-TXP phenol binds externally, DHP uses $H_2O_2$ as a cosubstrate to oxidize 2,4,6-TXP into a 2,6-DXQ, which spontaneously oxidizes further in aqueous solution.[17,19] However, peroxidase activity can be inhibited by the binding of a 4-halophenol in the internal inhibitor-binding site.[12] The presence of an internal binding site is unique to DHP, distinguishing it from other globins, which lack substrate-binding sites entirely. On the other hand, heme peroxidases typically bind substrates externally.[20] In DHP, the internal inhibitor-binding site has a unique two-site competitive binding mechanism, in which the internal and external binding

**Received:** May 17, 2014
**Revised:** October 19, 2014
**Published:** October 20, 2014





dx.doi.org/10.1021/bi5005975 | *Biochemistry* 2014, 53, 6863−6877

sites communicate through two conformations of the distal histidine of the enzyme, resulting in nonclassical competitive inhibition.[12] The internal cavity accommodates larger halogens better than smaller atoms in the para position of the phenolic inhibitor with the binding constants decreasing in the following order: I > Br > Cl > F.[12] X-ray crystallography shows that 2,4,6-TBP and 2,4,6-TCP can also bind internally in a binding site separate from where the *p*-halophenol binds.[15,16] The internal binding of the substrate may compete with external binding, have a different function, or even inhibit peroxidase activity.[16] Two studies have shown that DHP catalytic activity is inhibited at high substrate concentrations, which we attribute to substrate inhibition.

Although extensive research has been dedicated to the enzymatic activity and mechanism of DHP, there has been no study of protein stability with respect to heme loss, which in turn can affect enzymatic activity. Enzymatic activity requires a balance between structural flexibility and stability. Locally unfolded or disordered regions of a protein structure allow efficient interactions with binding partners, which can help to regulate cellular pathways. The active sites of enzymes and binding sites of proteins are a general source of instability because they contain groups that are exposed to solvent in order to bind substrates and ligands. Therefore, there is often a compromise between stability and activity in the structure of the protein active site.[21,22] If these two competing factors are optimized, it is possible that any increase in enzymatic activity can occur only at the expense of a decrease in folding stability. Application of this hypothesis to heme proteins suggests that greater access to the distal pocket associated with rapid substrate binding will increase the level of exposure of hydrophobic amino acids and the heme itself to solvent, which will tend to destabilize the heme. The combined effect of structural changes due to site-directed mutations on functional aspects, such as autoxidation rates and heme loss, has been studied extensively in sperm whale myoglobin (SWMb).[23] Heme loss is an irreversible process, which limits the rigorous thermodynamic interpretation of the data in terms of the folding stability of the apoprotein. Nonetheless, the relative heme loss temperatures and denaturant concentrations provide important information about the relative heme binding affinities of different forms of DHP compared to those of other myoglobins. For example, the apoglobin of DHP rapidly aggregates and precipitates so that it is not possible to study the folding transitions of the apoprotein. This behavior is quite different from that of SWMb, which has both a measurable folding transition for heme loss and several folding intermediates in the apoprotein.[24,25]

DHP has two isoforms, DHP A and DHP B, which have similar structures and are both capable of peroxidase chemistry.[26] Both isoforms contain 137 amino acid residues, but DHP B differs from DHP A at five positions: I9L, R32K, Y34N, N81S, and S91G (Figure 1).[3] DHP B has catalytic rate ($k_{cat}$) 3 times greater than that of DHP A as measured by stopped-flow kinetics.[27] DHP A has been the focus of many studies for many years, while DHP B has received attention more recently following its expression and crystallization in 2010.[26] It is of interest to determine the heme binding affinity of DHP A and DHP B as a means of studying the effect of protein stability on catalytic activity. Both DHP isoforms interact strongly with a number of different inhibitors and substrates. At this point, the principle peroxidase substrates and inhibitors have structurally characterized internal binding

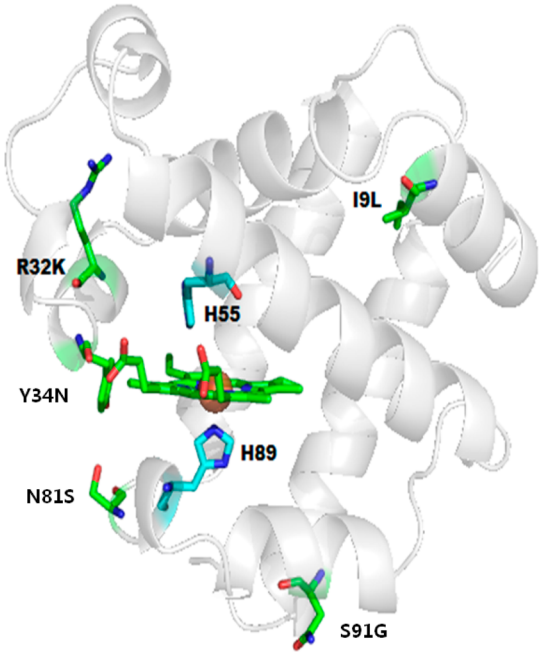


**Figure 1.** Key amino acid mutations that convert DHP A into DHP B. The five amino acid changes required to convert DHP A into DHP B are I9L, R32K, Y34N, N81S, and S91G.

sites.[10,12,15,16] Para-halogenated phenols act as inhibitors by binding internally in DHP and preventing the oxidization of trihalgonated phenols into dihalogenated quinones in the presence of $H_2O_2$.[12] The binding of 4-bromophenol results in inhibition by blocking the heme Fe and by pushing the distal histidine into an external conformation, which prevents it from playing an essential role as an acid–base catalyst. Para-halogenated phenol inhibitors serve a regulatory role in preventing the deleterious effects of radical generation when $H_2O_2$ is present without a substrate.[28] To understand the synergistic effects of inhibitor binding on protein structure, it is necessary to test the differential effect of these molecules on the stability of heme binding. Because ligand binding causes conformational changes in the structure, it may also play a role in determining the overall stability of the protein. To test this hypothesis, the thermal stabilities of various *p*-halophenol inhibitor–DHP complexes were studied by differential scanning calorimetry (DSC). Chemical denaturation was studied by the addition of denaturants such as urea and guanidnium hydrochloride (GdnHCl) and monitored by UV–visible spectroscopy. Because heme binding is stabilized by hydrophobic interactions in the interior of the globin, any change in the exposure to solvent or dynamic interaction with the addition of a ligand will change the entropy and enthalpy of the system, affecting the stability of the holoprotein.

## MATERIALS AND METHODS

All reagents were purchased from Aldrich and ACROS and used without further purification. 2,4,6-Trichlorophenol (2,4,6-TCP), 4-iodophenol (4-IP), 4-bromophenol (4-BP), 4-chlorophenol (4-CP), 4-fluorophenol (4-FP), and phenol were each dissolved in 100 mM, pH 7.0 potassium phosphate ($KP_i$) buffer to prepare the stock solution. Wild-type His6X (histidine-tagged) DHP was expressed in *Escherichia coli* and purified as previously described.[29,30] Ferric DHP was oxidized by excess $K_3[Fe(CN)_6]$ and then filtered through a NAP-25


dx.doi.org/10.1021/bi5005975 | *Biochemistry* 2014, 53, 6863–6877

column to eliminate excess $K_3[Fe(CN)_6]$ prior to each experiment. The concentrated protein stock solution was filtered through a 0.45 $\mu$m filter syringe membrane to remove any precipitants that may have formed during purification and concentration of the protein sample.

Apomyoglobin was prepared using the cold acid−butanone method described by Teale.[31] Myoglobin was adjusted to pH 2.0 by addition of HCl. The solution was moved to a separation funnel; an equal volume of 2-butanone was added, and the top aqueous layer was removed. Protein samples were dialyzed extensively at 4 °C against 3 × 5 L of 10 mM potassium phosphate (at intervals of 12 h and 24 h) at pH 7.0 to remove dissolved ketone. The apoprotein was then centrifuged to remove precipitate. Protein concentrations were determined using the following extinction coefficients: apomyoglobin, $\varepsilon_{280}$ = 15900 $\mu$M cm$^{-1}$;[32,33] DHP A and DHP B, $\varepsilon_{406}$ = 116400 $\mu$M cm$^{-1}$; DHP A H55V, $\varepsilon_{393}$ = 121304 $\mu$M cm$^{-1}$. The extinction coefficient for HSMb at 409 nm is 188000 $\mu$M cm$^{-1}$.

**Chemical Denaturation Using GdnHCl or Urea.** For all chemical denaturation experiments, a series of urea and GdnHCl concentrations were titrated into a sample that contained 10 $\mu$M protein in 100 mM, pH 7.0 $KP_i$ buffer. Protein samples were equilibrated with different concentrations of urea or GdnHCl for 24 h at room temperature for denaturant-induced unfolding studies. The Soret band of ferric DHP A at 407 nm was monitored using an Agilent 8453 diode array UV−visible spectrophotometer equipped with a thermostated cell. Before the absorption spectra were recorded, the samples were allowed to incubate for 3 min in a quartz cuvette placed in the thermal cell to reach thermal equilibrium.

Assuming the native state unfolds with high cooperativity, we hypothesize that a two-state model applies to protein denaturation from the native state, N, to the denatured state, D, with no significant intermediates. Then the unfolding (folding) equilibrium can be described as

$$N \rightleftharpoons D$$

The denaturation curve can be divided into three regions on the basis of absorbance change.[34,35] These three regions are (a) the pretransition region, in which the absorbance at 407 nm of folded protein changes slowly with denaturant concentration, (b) the transition region, which shows major variation of the physical parameter as unfolding proceeds, and (c) the post-transition region, which indicates slow changes in the physical parameter of the unfolded protein. In the case of DHP, attempts to extract the heme and purify apo-DHP via the cold acid−butanone method resulted in rapid aggregation and precipitation so that there is no current means to study the folding states of the apoprotein, Therefore, in the case of DHP, heme loss leads to immediate denaturation. Denaturation data are plotted in terms of denatured fractions, $f_D$, in which

$$f_D = \frac{Y - Y_N}{Y_D - Y_N} \quad (1)$$

where $Y$ is the observed absorbance at a given denaturant concentration and $Y_N$ and $Y_D$ are the extrapolated absorbances from the pre- and post-transition regions, respectively. Given that the unfolding reaction at the transition region is reversible, an equilibrium constant, $K_D$, can be calculated by determination of the denatured fraction of protein, $f_D$.

$$K_D = \frac{f_D}{1 - f_D} \quad (2)$$

On the basis of the equilibrium constant, the Gibbs free energy for protein unfolding at each denaturant concentration can be determined.

$$\Delta G_D = -RT \ln(K_D) \quad (3)$$

The plot of unfolding free energy as a function of denaturant concentration is extrapolated to 0 M to give the value of the unfolding free energy in the absence of denaturant, $\Delta G_D(H_2O)$.

$$\Delta G_D = \Delta G_D(H_2O) + m[\text{denaturant}] \quad (4)$$

The comparison of the denaturation of DHP A and B serves to provide a link between the folding stability and enzymatic activity. It is of particular interest to understand the influence of the native substrate, 2,4,6-TBP, on folding stability. Previous studies have used methanol (MeOH) as a cosolvent to increase the solubility of 2,4,6-TBP. Although the use of MeOH can increase the solubility of certain substrates, MeOH interferes only slightly with peroxidase function. Because this may be a complicating factor in a folding study, we investigated alternative methods for preparing substrate solutions at concentrations sufficient for the studies to be conducted. We found that heating solutions of 2,4,6-TBP to the boiling point followed by gradual cooling increased the solubility ~3−4-fold. Saturated (and perhaps supersaturated) solutions of 2,4,6-TBP prepared at higher temperatures contain a concentration of 2,4,6-TBP higher than the concentration that has been achieved in previous studies in aqueous buffer solutions. Therefore, equilibrium can be reached in a 24 h time span for kinetic measurements. This study allows comparison between the DHP A and DHP B catalytic efficiency of both TCP and TBP in the absence of MeOH and the effects of substrate inhibition relative to protein stability.

**Thermal Denaturation.** Heat-induced denaturation was studied using two instruments, a UV−visible spectrophotometer and TA Instruments Q100 temperature-modulated differential scanning calorimeter. The Soret band of DHP was measured using an Agilent 8453 diode array UV−visible spectrophotometer equipped with a thermostatic quartz cuvette covered with a lid to prevent evaporation. Protein concentrations were 10 $\mu$M for all measurements with a temperature range from 20 to 60 °C. Samples were incubated at 20 °C for 5 min followed by measurement at 1 °C increments every 2 min.

For DSC studies, the protein concentration was 3 mM for all measurements in high-volume volatile aluminum sample pans in 50 $\mu$L aliquots, sealed with a rubber O-ring. A sample pan with degassed buffer was used as the reference, and degassed buffer was used to dilute the sample to the appropriate concentration. Each sample was equilibrated to 20 °C for 5 min and then the temperature modulation applied (±0.5 °C per 60 s). The DSC curves were obtained using a scanning rate of 2 °C min$^{-1}$ from 20 to 100 °C. The temperature at the endothermic peak is used to represent the midpoint melting temperature ($T_m$). Data were collected in an Excel worksheet and analyzed using Igor Pro 6.0. The two-state denaturing model was used to fit the experimental measurement DSC curve to obtain corresponding $\Delta H_{vH}$, $\Delta H_{cal}$, and $T_m$ values. The baseline was also calculated on the basis of this model. The detailed description of the model construct and fitting is presented in the Supporting Information.


dx.doi.org/10.1021/bi5005975 | Biochemistry 2014, 53, 6863−6877

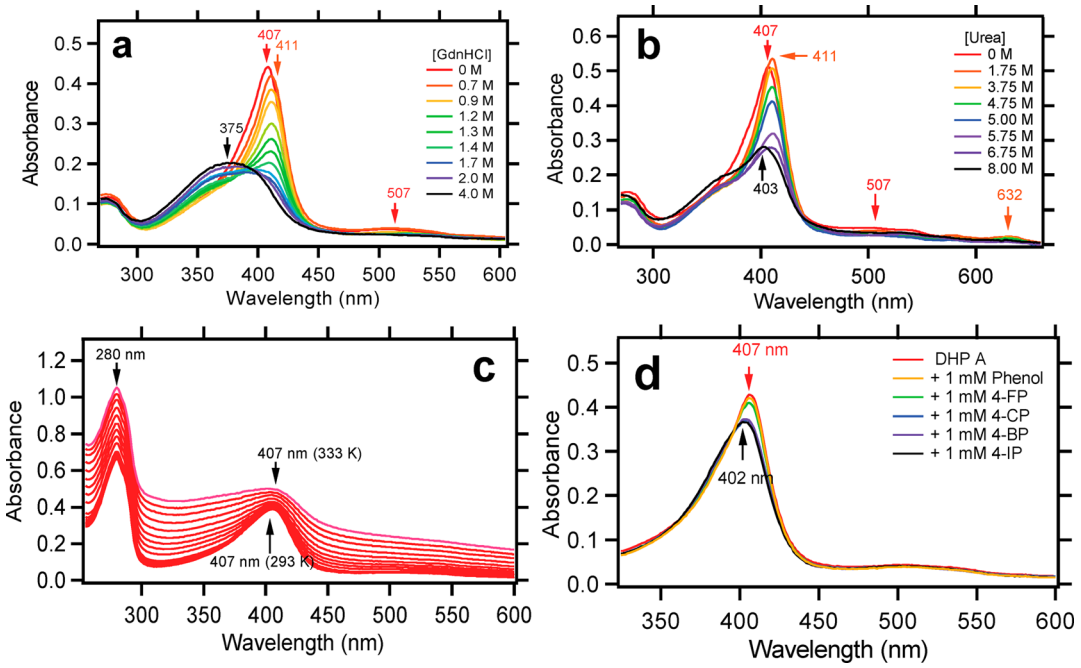


**Figure 2.** (a) Spectral changes of DHP A upon titration with GdnHCl. The protein concentration was 10 $\mu$M at pH 7.0 in 100 mM potassium phosphate buffer. (b) Spectral changes of DHP A upon titration with urea under the same conditions. (c) Spectral changes of DHP A determined by UV−visible thermal denaturation from 20 to 60 °C in the presence of 1 mM 4-BP under the same conditions. The "transition point" is the point of lowest absorbance before an exponential increase in absorbance. (d) Spectral changes of DHP A with different para-substituted phenols at a concentration of 1 mM.

**Heme Transfer.** Heme transfer was measured by observing the absorbance change at 407 nm associated with transfer of heme from holoprotein to excess apomyoglobin. Heme transfer experiments were conducted in 100 mM $KP_i$ buffer at pH 7 and 25 °C. Protein samples were incubated for 3 min at 25 °C followed by the addition of apomyoglobin (horse skeletal muscle) with 1 s intervals between each measurement. Rate constants for heme loss, $k_1$ and $k_2$, were obtained from fits of each time course to a double-exponential expression. The data were normalized by subtracting a baseline at $A_{407}$ to obtain the observed $\Delta A_{407}$.

**Kinetic Assays.** Data from the time course spectrum were first fit to a linear function to obtain the initial reaction velocity at a given substrate concentration. Because DHP B has a faster reaction rate, only the first four points (0−3 s) were in the linear range. The kinetic assays were conducted in a 0.4 cm path length quartz cuvette with a total volume of 1200 $\mu$L. To reach thermal equilibrium, DHP and the substrate were allowed to incubate for 3 min in the cuvette placed in the thermal cell. The $H_2O_2$ solution was injected into the cuvette within 1 s of initiation of data collection.

## RESULTS

**Absorption Spectroscopy.** The spectral changes shown in Figure 2a−d indicate three factors that can influence the Soret absorption band, which is observed at 407 nm in the wild-type DHP A and B ferric form. The ferric form is known from X-ray crystallography and resonance Raman spectroscopy to be a 40/60 mixture of 5-coordinate high spin (5cHS) and 6-coordinate high spin (6cHS) forms with water bound to the heme iron.[11,12] Chaotrophic agents, ligand binding, and temperature modifications perturb the system, causing shifts in the Soret band. The effect of the addition of inhibitors, such as 4-BP, is to displace the $H_2O$ molecule from the heme iron, thereby causing the population to shift toward the 5cHS form, which leads to a shift of the Soret band from 407 nm to a lower wavelength.[11,12] Spectra of ferric DHP A clearly show this phenomenon upon addition of a series of para-halogenated phenols (Figure 2d). Phenol, which is a well-known denaturant, was used as a control for comparison to the series of para-halogenated phenols in terms of the perturbing effect on the Soret band. The series of para-halogenated phenols have been observed to obey a trend that the binding affinity and inhibitory activity correlate with the increasing size of the halogen atom. Phenol has the weakest binding, and the binding constant increases as the radius of the para halogen atom increases.[12] These para-halogenated phenols act primarily as DHP inhibitors with the exception of 4-fluorophenol and phenol, which also act as substrates. However, phenol and halogenated phenols are also denaturants, and thus, the nonspecific effects that decrease the level of protein structure are expected at higher concentrations.

The GdnHCl concentration-dependent UV−visible spectra clearly show that heme loss is taking place. At the beginning, the Soret band of DHP A shifted from 407 to 411 nm, which may suggest the binding of GdnHCl to the heme. As the concentration of GdnHCl increases, the intensity of the Soret band starts to decline, indicating heme loss due to rupture of the coordination of heme iron to the proximal histidine.[24] Eventually, the Soret band disappeared and was replaced by a broader band centered at 375 nm. However, the urea concentration-dependent UV−visible spectra are quite different from those of GdnHCl. Initially, the Soret band also shifted from 407 to 411 nm, and the Soret band becomes sharper, which indicates the formation of the 6cHS form with a urea carbonyl group coordinated to the heme. Then the intensity of the Soret band also rapidly declined, as it shifted to 403 nm by the end of the titration.


dx.doi.org/10.1021/bi5005975 | *Biochemistry* 2014, 53, 6863−6877

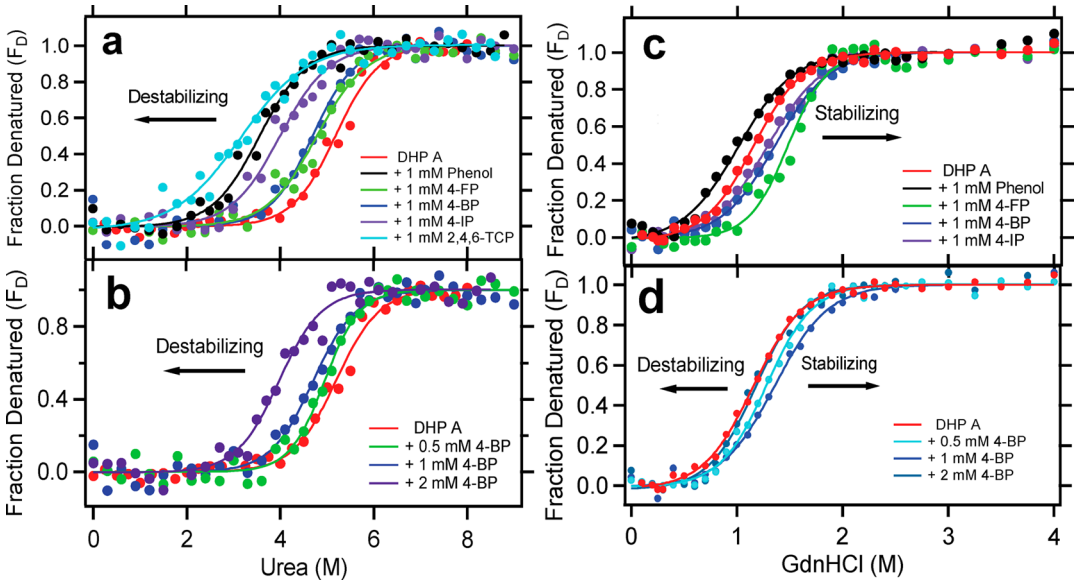


**Figure 3.** (a) Fractional degree of denaturation of DHP A as a function of urea monitored by the change in absorbance with increasing concentrations of 4-BP. (b) Urea with addition of phenol, 4-XP, and 2,4,6-TCP. (c) Fractional degree of denaturation of DHP A as a function of GdnHCl monitored by the change in absorbance with increasing concentrations of 4-BP. (d) GdnHCl with addition of phenol and 4-XP.

**Chemical Denaturation.** The Soret band was monitored in the chemical denaturation experiments as an indicator of the degree of heme dissociation. In this section, we focus on the study of the synergistic effect of the binding of para-substituted phenols with the chemical denaturation induced by GdnHCl and urea. Figure 3 shows the denaturation curves of DHP A with urea and GdnHCl. The observed trend for urea is an additive destabilizing effect leading to an increased level of destabilization by the para-halogenated phenols. Two different mechanisms have been proposed for the urea-induced unfolding of protein. The indirect mechanism hypothesizes that urea disrupts the water structure in the protein and facilitates exposure of the hydrophobic pocket. The direct mechanism suggests that the binding of urea leads to solvation of the polypeptide chain, which causes it to lose secondary structure.[36−38] As shown in panels a and b of Figure 3, all urea-treated samples were destabilized to an extent proportional to the concentration of para-halogenated phenol.

Panels c and d of Figure 3 show that a different trend is observed when GdnHCl is used as the denaturant. Except for phenol, all halogenated phenols stabilize the protein in the presence of GdnHCl by binding in the distal pocket when they are present at concentrations of <1 mM. One explanation for this observation is that the protein−ligand complex rigidifies and stabilizes the globin. In a similar way, the highest-resolution X-ray crystal structures of DHP are those that have 4-BP bound in the distal pocket.[12,39] This may also lead to a protection of the globin from attack by the denaturant in the distal pocket. These mechanisms will be considered in the discussion below. The stabilization effect upon para-halogenated phenol binding is shown in Table 1 based on the calculated $\Delta G_D(H_2O)$ value (Figure 4). The relative stabilization by the para-halogenated phenols at <1 mM changes to a destabilization at higher concentrations. Thus, at sufficiently high inhibitor concentrations, the synergistic effects are parallel for both urea and GdnHCl. Table 1 presents the results of the analysis of chemically mediated denaturation. 2,4,6-TCP resulted in the greatest destabilization of any substrate tested, which decreased $urea_{1/2}$ and $\Delta G_D(H_2O)$ by a factor of ∼4 relative to those with

**Table 1. Summary of Chemically Mediated Unfolding for GdnHCl and Urea**

| | $\Delta G_D(H_2O)$ (kcal mol$^{-1}$) | $m$ (kcal mol$^{-1}$ M$^{-1}$) | $GdnHCl_{1/2}$ (M) |
|---|---|---|---|
| DHP A | 2.90 ± 0.08 | −2.51 ± 0.06 | 1.15 ± 0.01 |
| + 0.5 mM 4-BP | 3.02 ± 0.12 | −2.36 ± 0.09 | 1.28 ± 0.01 |
| + 1 mM 4-BP | 3.13 ± 0.07 | −2.30 ± 0.06 | 1.36 ± 0.02 |
| + 2 mM 4-BP | 2.73 ± 0.20 | −2.35 ± 0.15 | 1.18 ± 0.02 |
| + 1 mM 4-IP | 2.95 ± 0.11 | −2.28 ± 0.08 | 1.29 ± 0.02 |
| + 1 mM 4-FP | 4.32 ± 0.33 | −3.20 ± 0.23 | 1.48 ± 0.02 |
| + 1 mM phenol | 2.19 ± 0.09 | −2.19 ± 0.07 | 1.01 ± 0.02 |
| DHP B | 2.21 ± 0.15 | −1.99 ± 0.11 | 1.09 ± 0.02 |
| | $\Delta G_D(H_2O)$ (kcal mol$^{-1}$) | $m$ (kcal mol$^{-1}$ M$^{-1}$) | $Urea_{1/2}$ (M) |
| DHP A | 6.80 ± 0.85 | −1.31 ± 0.17 | 5.19 ± 0.05 |
| + 0.5 mM 4-BP | 6.43 ± 0.43 | −1.31 ± 0.09 | 4.95 ± 0.04 |
| + 1 mM 4-BP | 5.92 ± 0.28 | −1.26 ± 0.06 | 4.69 ± 0.05 |
| + 2 mM 4-BP | 5.13 ± 0.27 | −1.29 ± 0.07 | 3.97 ± 0.06 |
| + 1 mM 4-IP | 5.34 ± 0.71 | −1.30 ± 0.16 | 4.00 ± 0.06 |
| + 1 mM 4-FP | 6.29 ± 0.66 | −1.31 ± 0.13 | 4.79 ± 0.07 |
| + 1 mM phenol | 4.43 ± 0.26 | −1.23 ± 0.07 | 3.56 ± 0.05 |
| + 1 mM 2,4,6-TCP | 2.81 ± 0.19 | −0.89 ± 0.06 | 3.17 ± 0.09 |
| DHP B | 2.42 ± 0.14 | −0.62 ± 0.03 | 4.12 ± 0.14 |
| DHP A H55V | 7.52 ± 0.98 | −1.44 ± 0.19 | 5.35 ± 0.36 |

1 mM 4-BP. The GdnHCl denaturation midpoint, $GdnHCl_{1/2}$, is ∼3−4 times lower than that of urea, $urea_{1/2}$, indicating that it is a stronger denaturant. Urea denaturation and GdnHCl denaturation produced different results in the presence of the para-halogenated phenols. For urea denaturation, 1 mM para-halogenated phenols destabilized DHP A, but for GdnHCl denaturation, 1 mM para-halogenated phenols stabilized DHP A. Increasing the concentration of 4-BP in the presence of GdnHCl resulted in destabilization, which caused $GdnHCl_{1/2}$ to decrease from 1.36 ± 0.02 in 1 mM 4-BP to 1.18 ± 0.02 in 2 mM 4-BP. Therefore, there is a threshold of stabilization in GdnHCl with a lower ligand concentration, and destabilization occurs at a higher ligand concentration. For both urea and


dx.doi.org/10.1021/bi5005975 | Biochemistry 2014, 53, 6863−6877

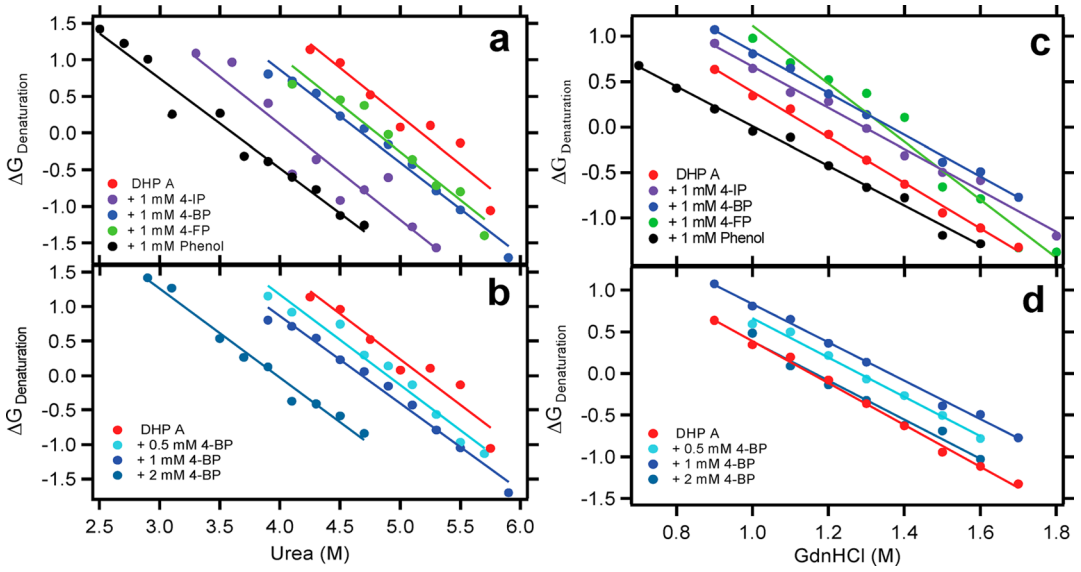


**Figure 4.** Least-squares fitting for DHP unfolding as a function of urea and GdnHCl concentration to calculate $\Delta G_D(H_2O)$.

GdnHCl denaturation, the data are consistent with the idea that halophenol decreases the stability of proteins with an increase in the size of the halogen substitute (4-IP > 4-BP > 4-FP). Finally, the chemical denaturation experiments using GdnHCl and urea both showed that DHP B is much less structurally stable than DHP A, yet the two isoforms are differentiated by only five of 137 amino acids (Figure 5).

**Thermal Denaturation.** We applied DSC to determine the enthalpy $\Delta H$ and transition temperature $T_m$ of the thermal unfolding of DHP A and DHP B in the presence of the internal binding inhibitor. The DSC experimental curve was fit based on the two-state unfolding model to determine $\Delta H_{vH}$, $\Delta H_{cal}$, and $T_m$ (Table 2). The fitting procedure for the DSC curve is presented in Figure S1 of the Supporting Information. Repeated scans of the denatured samples showed a flat baseline and no melting profile on the second thermal scan, indicating that thermal denaturation occurs irreversibly. Figure 6a shows DHP A and DHP B each have a single endothermic peak at 50.4 °C (323.4 K) and 47.5 °C (320.5 K), respectively. In addition, increasing concentrations of 4-BP shifted the endothermic peak to the lower melting temperature and slightly decreased peak intensity. Every 1 mM change in 4-BP concentration decreases the $T_m$ by ~0.6 K, which suggests that 4-BP decreases the thermal stability of the protein upon binding. The summary of DSC data is shown in Table 1.

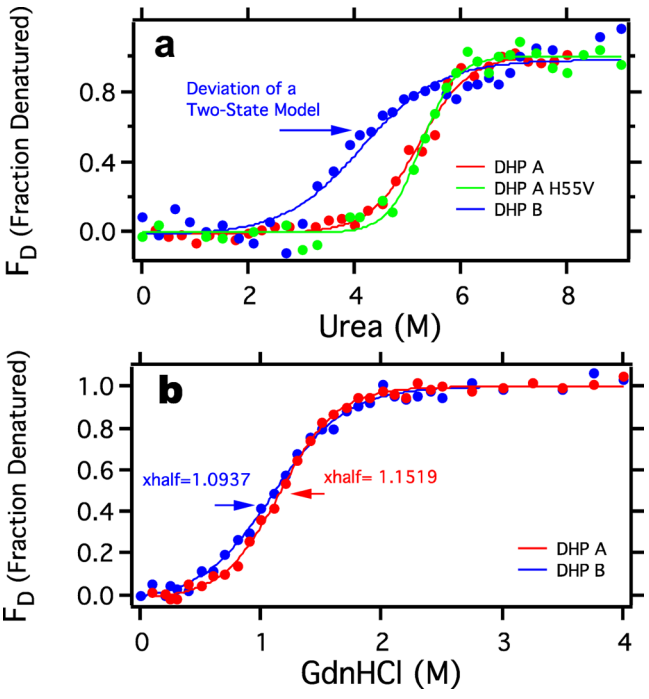


**Figure 5.** (a) Urea chemical denaturation comparison between DHP A and DHP B fitted with a sigmoidal curve fitting. (b) GdnHCl chemical denaturation comparison between DHP A, DHP B, and H55V fitted with a sigmoidal curve fitting.

**Table 2. DSC Data for the Thermal Unfolding of DHP**

| | $\Delta H_{cal}$ (kJ/mol) | $\Delta H_{vH}$ (kJ/mol) | $T_m$ (°C) |
|---|---|---|---|
| DHP A | 183.3 | 383.8 | 50.5 |
| DHP B | 165.1 | 335.7 | 47.7 |
| DHP A + 1 mM 4-BP | 163.1 | 411.5 | 49.8 |
| DHP A + 3 mM 4-BP | 166.0 | 396.4 | 48.6 |

For a two-state denaturation process to occur, the ratio between $\Delta H_{vH}$ and $\Delta H_{cal}$ should be equal to 1. However, the calculated values of $\Delta H_{vH}$ for DHP A and DHP B are twice the experimental values of $\Delta H_{cal}$, indicating the formation of an intermediate during the unfolding process. A large $\Delta H_{vH}$ may result from reactions having small calorimetric enthalpy changes and irreversible unfolding.[40,41] The addition of 4-BP to DHP A further increases the discrepancy between the van't Hoff and calorimetric enthalpies by increasing the $\Delta H_{vH}$, while decreasing the $\Delta H_{cal}$. Cytochrome *c* peroxidase has shown a $\Delta H_{vH}/\Delta H_{cal}$ ratio of 2, as well.[41]

Both thermal denaturation studies (through DSC and UV–vis) show that DHP A is more thermally stable than DHP B. Examination of protein folding stability in the presence of inhibitors and substrates adds an additional factor because ligands bind to native or non-native states with different binding strengths. Taking heme loss ($K_{-H}^{NH}$ and $K_{-H}^{UH}$) into consideration and assuming that a ligand may interact with the


dx.doi.org/10.1021/bi5005975 | *Biochemistry* 2014, 53, 6863–6877

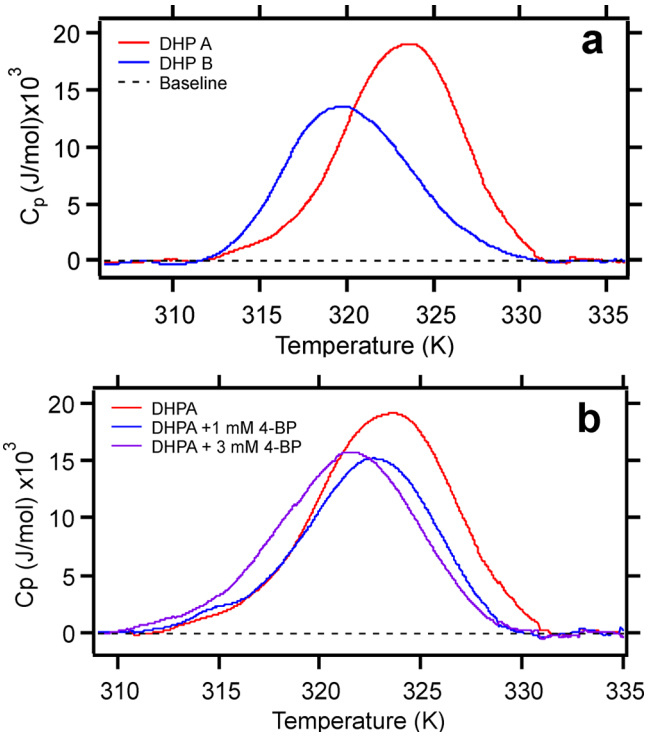


**Figure 6.** (a) Differential scanning calorimetry scans of DHP A and DHP B at 3 mM protein. (b) Differential scanning calorimetry scans of DHP A with increasing concentrations of 4-BP.

native state (NH) or a particular non-native/unfolded conformation (UH), the DHP denaturation scheme is shown in Scheme 1, in which $K_L^X$ (X = NH, N, UH, or U) values are

**Scheme 1. DHP Denaturation Mechanism in the Presence of Binding Ligands**

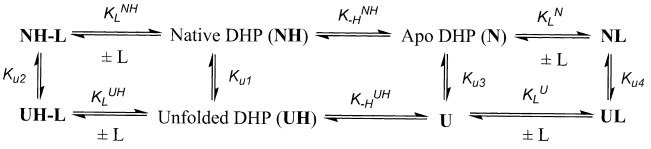


the equilibrium binding constants for the native and non-native state with and without cofactor heme, respectively. $K_{ux}$ ($x$ = 1, 2, 3, or 4) is the unfolding equilibrium constant. An unfolded state of the holoprotein may have a portion of the heme exposed to the solvent due to local loss of secondary structure. High phenolic ligand concentrations can induce unfolding by lowering the stability of the hydrophobic core, which drives the protein to unfold. Once they are partially unfolded, we propose that para-halogenated phenols and trihalophenols facilitate heme loss, which leads to complete denaturation of DHP, as discussed above. DSC data in Figure 6b support the hypothesis that 4-BP binding causes destabilization, a decrease in folding free energy, and a decrease in $T_m$. Multiple sites of binding could further increase the population of non-native states relative to that of the native state. Thus, at the high concentration of halogenated phenol, native DHP starts to denature, which results in the decrease in the catalytic rate observed in the kinetic assay (Figures 9 and 10).

Figures 2c and 7 show the thermal denaturation profile of DHP through temperature-controlled UV−visible spectroscopy. The data deviate from a two-state transition model, which is

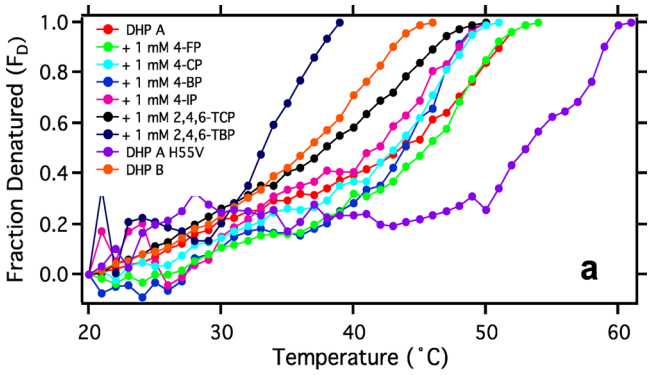


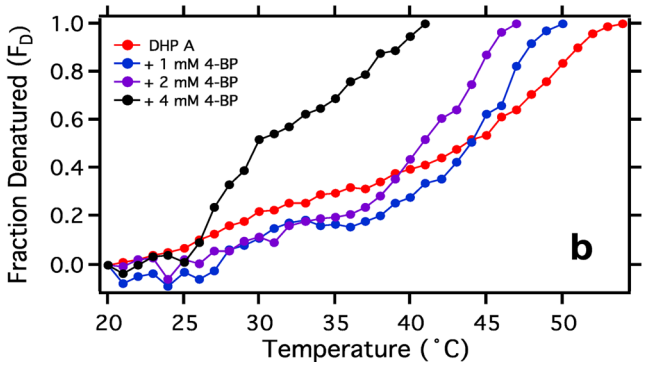


**Figure 7.** (a) Comparison of thermal denaturation between para-halogenated and trihalogenated phenols. (b) Thermal denaturation with increasing concentrations of 4-BP.

consistent with the DSC data discussed above. Equation 1 was used to normalize the data with $Y_N$ as the absorption at 20 °C and $Y_D$ as the lowest absorption. Beyond that maximum point of each curve (lowest absorption), the absorbance started to increase exponentially over time even when the temperature was not increased. In addition, the sample in the cuvette appeared cloudy, indicating that the protein may have been completely denatured by this point. Because the data deviate from a two-state model, a pre- and post-transitional region could not be determined to accurately calculate the enthalpy and $T_m$ of denaturation. Nevertheless, the data appear to be in agreement with data from DSC and chemical denaturation studies. The maximum in DSC thermal scans associated with phase transitions can be called the melt temperature, $T_m$. Table 3 shows $T_m$ values for the phase transition for each curve.

**Table 3. Transition Points for Temperature-Controlled UV−Visible Spectroscopy Denaturation**

| | $T_m$ (°C) |
|---|---|
| DHP A | 54 |
| DHP B | 46 |
| DHP A H55V | 61 |
| DHP A + 1 mM 4-FP | 54 |
| DHP A + 1 mM 4-CP | 51 |
| DHP A + 1 mM 4-BP | 50 |
| DHP A + 2 mM 4-BP | 47 |
| DHP A + 4 mM 4-BP | 41 |
| DHP A + 1 mM 4-IP | 51 |
| DHP A + 1 mM 2,4,6-TCP | 50 |
| DHP A + 1 mM 2,4,6-TBP | 39 |


dx.doi.org/10.1021/bi5005975 | Biochemistry 2014, 53, 6863−6877

Because precipitation occurs above this temperature, these values do not correspond to reversible thermodynamic quantities but rather are only qualitative due to irreversibility.

The binding of ligands alters the transition temperature, thus implying changes in stability against denaturation. With every 1 mM change in the concentration of 4-BP added, the transition temperature decreases ~3 °C, showing that increasing concentrations of 4-BP destabilize the protein. The limited solubility of TXP's prevents it from being used in DSC studies, but the solubility is high enough for UV−visible spectroscopy temperature studies. The trihalogenated phenols 2,4,6-TBP and 2,4,6-TCP are among the strongest destabilizing ligands for protein folding and have a much greater destabilizing effect than para-halogenated phenols.

**Heme Transfer.** Using three variants (DHP A, DHP B, and the H55V mutant of DHP A), the relative strength of binding of heme to DHP was examined by measuring the kinetic rate of heme transfer from DHP to excess horse skeletal muscle apomyoglobin. Heme transfer occurs because apomyoglobin has a high heme affinity compared to that of holo-DHP-hemoglobin.[23,24,42,43] A spectral shift occurs from the 407 nm region to the 409 nm region where holo-DHP-hemoglobin[44] ($\varepsilon_{409}$ = 188000 $\mu$M cm$^{-1}$) has an extinction coefficient higher than that of DHP ($\varepsilon_{406}$ = 116400 $\mu$M cm$^{-1}$). Both the increase in absorbance and the 2 nm shift are indications that holomyoglobin was formed. Figure 8a shows the spectral shift in DHP A over the course of 11 h. Figure 8b shows the change in absorbance associated with heme transfer for DHP A, after addition of ligands DHP A, DHP B, and H55V. The H55V mutation in DHP A was used to test whether decreasing the polarity of the interior heme pocket reduces the heme binding affinity of DHP as observed for SWMb.[44]

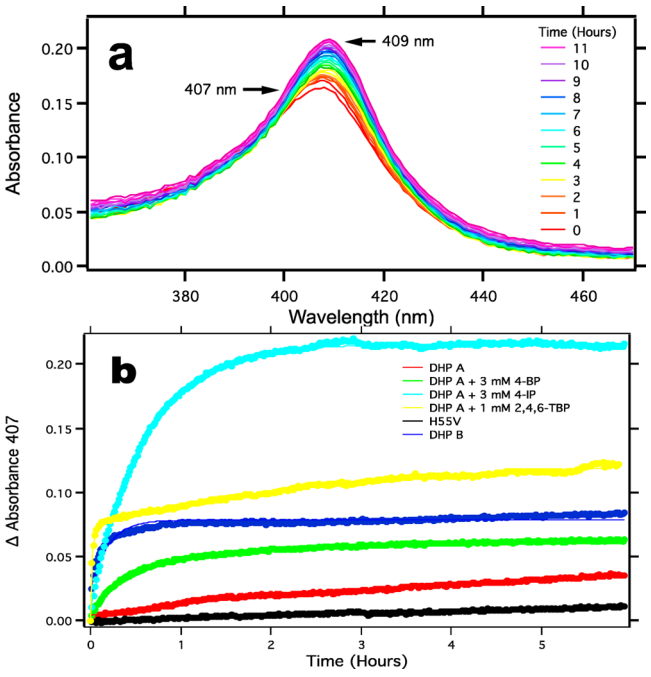


**Figure 8.** (a) Absorbance spectrum of 3 $\mu$M DHP A supplemented with 30 $\mu$M apomyoglobin incubated at 25 °C for 11 h. The increase in absorbance at 407 nm and the shift to 409 nm are characteristic of holomyoglobin formation. (b) Time course of the change in absorbance at 407 nm of DHP A, H55V, and DHP B and addition of phenolic ligands. Each curve is fitted to a double-exponential curve.

Heme transfer from DHP to apomyoglobin follows a biphasic behavior (a fast phase followed by a slow phase) and was fitted with a double-exponential expression. The heme must migrate out of one pocket into water and from water into another pocket. The fast phase could be associated with the removal of the heme, and the slow phase could be associated with a slow heme rearrangement and/or coordination in myoglobin.[45] The observed heme binding rate constants, $k_1$, parallel the protein stability and increase in the following order: H55V < DHP A < DHP B. The magnitude of $k_1$ is larger for DHP B than for DHP A by a factor of ~43. The H55V mutant has a $k_1$ ~22-fold lower than that of DHP A, indicating that nonpolar residues in the distal pocket tend to stabilize the heme in the distal pocket and increase the barrier for heme extrusion. The subtle changes in protein structure in DHP B accelerate heme loss in the heme transfer experiments (Table 4). These experiments corroborate the idea that heme is more strongly bound in DHP A than in DHP B. The addition of a halogenated phenol increases the rate of heme dissociation by desolvation. The addition of 3 mM 4-BP increased $k_1$ by a factor of ~14. Larger phenols (2,4,6-TBP) could facilitate water loss and help sterically push the heme out. Therefore, lower concentrations of 2,4,6-TBP are required to cause heme dissociation compared to those of 4-BP.

**Table 4. Rate Constants of Heme Transfer from DHP to Apomyoglobin**

| | $k_1$ (h$^{-1}$) | $k_2$ (h$^{-1}$) |
|---|---|---|
| DHP A | 0.237 | 0.237 |
| DHP B | 10.230 | 0.118 |
| DHP A H55V | 0.011 | 0.011 |
| DHP A + 3 mM 4-BP | 3.361 | 0.487 |
| DHP A + 1 mM 2,4,6-TBP | 46.626 | 0.335 |

**Kinetics.** The method of forming a saturated solution of 2,4,6-TBP by heating to the boiling point permitted us to compare the kinetics of oxidation of 2,4,6-TCP and 2,4,6-TBP by DHP without the addition of nonaqueous solvents (e.g., MeOH) used in previous work.[15] The kinetic data in Figures 9a and 10a show the concentration range of 2,4,6-TBP and 2,4,6-TCP that follows Michaelis−Menten kinetics, while Figures 9b and 10b show kinetics at higher substrate concentrations where substrate inhibition occurs. The data were fitted with the modified Michaelis−Menten diffusion model.[15] Varying protein

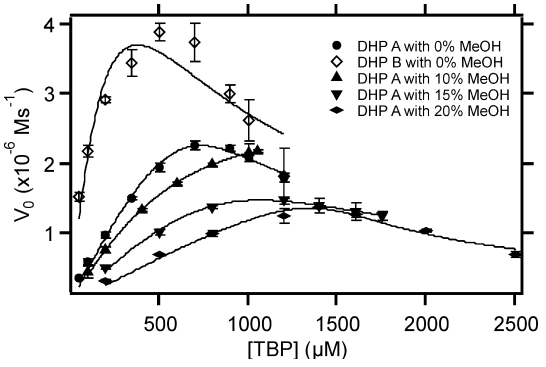


**Figure 9.** Single-wavelength kinetics of DHP-catalyzed 2,4,6-TBP oxidation as a function of substrate concentration with DHP A and DHP B showing increasing concentrations of organic solvents (i.e., MeOH) decrease catalytic activity.


dx.doi.org/10.1021/bi5005975 | Biochemistry 2014, 53, 6863−6877

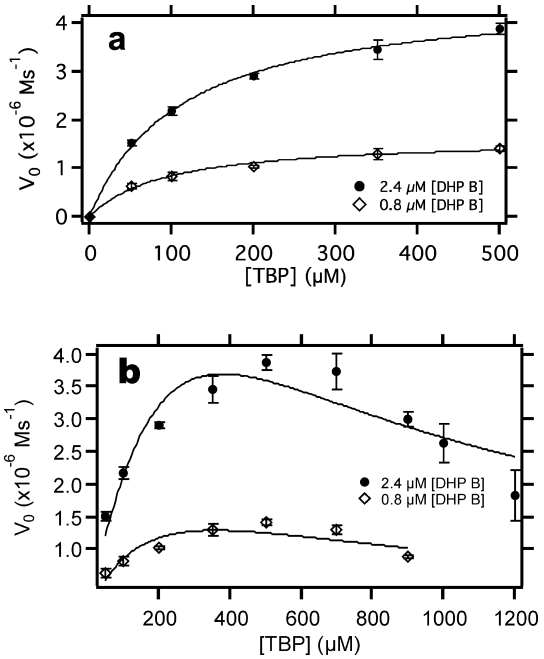


**Figure 10.** Single-wavelength kinetics of (a) DHP B-catalyzed 2,4,6-TBP oxidation as a function of substrate concentration fitted with the Michaelis–Menten equation and (b) DHP B fitted with the substrate inhibition model at higher concentrations.

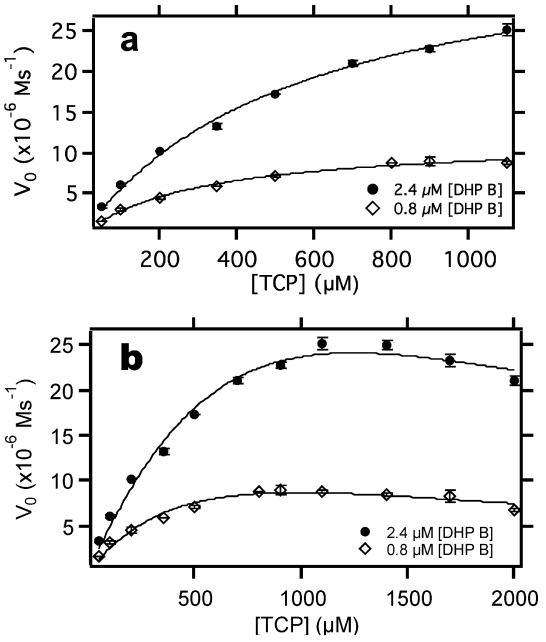


**Figure 11.** Single-wavelength kinetics of DHP-catalyzed 2,4,6-TCP oxidation as a function of substrate concentration (a) fitted with the Michaelis–Menten equation and (b) fitted with the substrate inhibition model at higher concentrations.

concentrations were used to observe the effects on the $K_m$ and maximal substrate concentration before a decline in the catalytic rate. Overall, our data are consistent in showing that DHP B has a catalytic activity greater than that of DHP A. At pH 7, the DHP B:DHP A rate ratios are ~5- and ~6-fold for 2,4,6-TCP and 2,4,6-TBP, respectively. This difference in enzymatic rate is even greater than that in previous reports obtained using stopped-flow kinetics.[26] The origin of the difference may be that previous studies held 2,4,6-TXP substrate concentrations constant while cosubstrate $H_2O_2$ concentrations were varied. The method used here was to vary the 2,4,6-TXP substrate concentrations and hold $H_2O_2$ concentrations constant. Using the classical Michaelis–Menten method of varying the substrate concentration, we observe that $k_{cat}$ for oxidation of 2,4,6-TBP for both DHP A is DHP B is nearly the same. The origin of the increase in enzymatic rate in DHP B is mainly an ~6-fold smaller $K_m$ for DHP B. This suggests that the on rate for substrate binding is significantly enhanced in DHP B, which in turn is related to the hydrophobicity of surface pockets where the substrate must bind for peroxidase function.

When DHP catalyzes 2,4,6-TCP or 2,4,6-TBP, substrate inhibition occurs in DHP B at a lower concentration than in DHP A, resulting in a lower $K_I$ for DHP B. Figure 10b shows that a maximal rate of oxidation of 2,4,6-TBP is reached at a substrate concentration of ~500 μM for both 2.4 and 0.8 μM protein. Figure 11b shows that the DHP B turnover frequency of 2,4,6-TCP reaches a maximum at ~1400 and ~1100 μM/min at 2.4 and 0.8 μM protein, respectively. The data show that 2.4 μM DHP B reaches a maximal catalytic rate for both TBP and TCP in $KP_i$ buffer sooner than DHP A. DHP A reaches a maximal catalytic rate for TCP at ~2000 and ~700 μM/min for 2,4,6-TBP.[15] Tables 5 and 6 summarize the Michaelis–Menten fitting parameters. In Figure 9, we show a comparison between DHP oxidation of 2,4,6-TBP in the presence of MeOH. The data are consistent, showing that catalytic efficiency decreases with increasing concentrations of MeOH, which will be explained below.

There is also an optimal $H_2O_2$:DHP ratio that prevents side reactions such as formation of compound RH.[46] For example, the catalytic efficiency of DHP B for 2,4,6-TCP and 2,4,6-TBP conversion decreases by ~25% as the protein concentration is increased from 0.8 to 2.4 μM. Although the kinetic model for the modified Michaelis–Menten rate scheme for peroxidases suggests a rate saturation behavior with parameters $V_{max} = k_1[H_2O_2][E]_0$ and $K_m = (1/k_2 + 1/k_3)k_1[H_2O_2]$, experimental observation suggests that side reactions due to a high $H_2O_2$ concentration actually slow the rate of product formation. Substrates can protect the protein from the harmful side reactions caused by $H_2O_2$ alone. Aside from the considerations of diffusion, which increase the second-order rate for formation of the ES complex, this protection by the substrate provides another reason why increases in substrate concentration result in a rate increase.

## DISCUSSION

This study was designed to test the relative heme binding affinity of DHP A and B and the effects of phenolic substrate and inhibitor binding. The heme plays a crucial role in structure–function relationships of hemoproteins, acting both as a catalytic center (binding site) and as a stabilizer of the native folded state. Coordination by water in the sixth position is also an important factor that may govern heme binding affinity. The fact that DHP A has only 50% bound $H_2O$ in the sixth coordination site (compared to 100% for ferric myoglobins studied) may be one reason for the decreased heme binding affinity of DHP. The role played by inhibitors and substrates may likewise be related to their tendency to exclude $H_2O$ from the distal pocket. These factors are also linked with the accessibility of the distal pocket, which in turn


dx.doi.org/10.1021/bi5005975 | Biochemistry 2014, 53, 6863–6877

Table 5. DHP Michaelis–Menten Kinetic Parameters for TBP

| | $V_m$ ($\mu$M s$^{-1}$) | $k_{cat}$ (s$^{-1}$) | $K_m$ ($\mu$M) | $k_{cat}/K_m$ (s$^{-1}$ mM$^{-1}$) |
|---|---|---|---|---|
| DHP A (2.4 $\mu$M) | 4.35 ± 0.33 | 1.814 ± 0.14 | 640.69 ± 83.50 | 2.83 ± 0.43 |
| DHP B (2.4 $\mu$M) | 4.63 ± 0.15 | 1.93 ± 0.06 | 110.6 ± 11.00 | 17.45 ± 1.82 |
| DHP B (0.8 $\mu$M) | 1.63 ± 0.08 | 2.04 ± 0.10 | 91.94 ± 16.20 | 22.18 ± 4.06 |

Table 6. DHP Michaelis–Menten Kinetic Parameters for TCP

| | $V_m$ ($\mu$M s$^{-1}$) | $k_{cat}$ (s$^{-1}$) | $K_m$ ($\mu$M) | $k_{cat}/K_m$ (s$^{-1}$ mM$^{-1}$) |
|---|---|---|---|---|
| DHP A (2.4 $\mu$M) | 19.40 ± 0.80 | 8.083 ± 0.33 | 1004.2 ± 90.0 | 8.045 ± 0.79 |
| DHP B (2.4 $\mu$M) | 39.62 ± 1.38 | 16.51 ± 0.58 | 425.42 ± 37.2 | 38.81 ± 3.66 |
| DHP B (0.8 $\mu$M) | 11.52 ± 0.51 | 14.40 ± 0.64 | 297.19 ± 35.1 | 48.45 ± 6.11 |

relates to the rate of activation of $H_2O_2$, substrate on rates, and therefore the overall enzymatic rate.

The relationship of heme binding to function is also of central interest in this study. Of course, once the heme is extruded, the protein immediately unfolds, resulting in a loss of biological activity. The loss of heme is related not only to bound $H_2O$ but also to distal pocket dynamics. DHP permits relatively large molecules (halogenated phenols) to bind in the distal pocket, which suggests a greater degree of dynamic motion than in typical myoglobins and hemoglobins. The internalization of phenols can have both stabilizing and destabilizing aspects. Despite the fact that phenols are known denaturants, the specific binding of the inhibitor 4-BP is known to significantly increase the resolution of the X-ray crystal structure in both wild-type DHP A and the L100F mutant of DHP A.[39] One reason for the preference for larger halogens in *p*-halophenols is that there is an internal Xe-binding cavity in DHP, which is where the halogen binds.[28] We have shown that the binding constants for the monohalophenols decrease in the following order: 4-IP > 4-BP > 4-CP > 4-FP.[12] One might consider that these observations indicate a net stabilization of the protein due to the binding of the inhibitor. However, para-halogenated phenols may indirectly cause denaturation by dehydration and desolvation as they interact with the enzyme. When 4-BP binds in the internal hydrophobic pocket (distal pocket), it displaces the water molecule bound to the heme Fe atom and displaces His55 into solvent. The conformation of His55 exposed to solvent is known as the open conformation. Normally, His55 is inside the distal pocket where it can interact with ligands bound to the heme Fe (closed conformation). The open conformation induced by binding of para-halogenated phenols is enthalpically disfavored but entropically favored.[47,48] The point is that the mechanism by which small molecules enter and exit the protein plays a role in the dynamics that lead to a decrease in folding stability.

Compared to unsubstituted phenol, the bromo group of 4-BP makes both the enthalpy and entropy of hydration more negative.[49] Halogenated phenols are stronger denaturants than phenol itself because of the increase in the level of dipole movement and stronger solute–solvent interaction with the addition of a halogenated group. On the basis of chemical and thermal denaturation studies by UV–visible spectroscopy and DSC, halophenols decrease the heme binding affinity and therefore also have an effect on protein stability. Moreover, the denaturing ability of halophenols increases with the size of the halogen (4-IP > 4-BP > 4-CP > 4-FP) and with the number halo substituents (2,4,6-TBP > 4-BP). Taken together, the data show that the interaction of the halogen atoms appears to be a double-edged sword. In some respects, the protein is stabilized by the interaction with an internal cavity, yet under denaturing conditions, an empirical correlation exists between the binding strength of the inhibitor and its capacity to denature the protein.

Our study suggests that urea and GdnHCl have different mechanisms of denaturation based on different peaks presented in the UV–visible spectrum (Figure 2a,b). GdnHCl-induced denaturation may cause full dissociation of the heme into apo-DHP, whereas urea may cause only partial dissociation of the heme, represented by the presence or absence of the 375 or 403 nm band, respectively. As a result, urea and GdnHCl have different estimates for the conformational stability of a protein.[50−54] Urea may function by an indirect effect that disrupts solvent structure near the protein. In this case, the denaturing effect of the *p*-halophenol is dominant. If, on the other hand, GdnHCl acts more directly by interacting with the solvent-exposed regions of the distal pocket, the binding of the inhibitor may act to compete with that binding and thereby stabilize the protein. As the *p*-halophenol concentration increases, a point at which the tendency of the phenol itself to denature the protein takes over is reached.

The studies of enzymatic rate as a function of substrate concentration reveal a non-Michaelis–Menten behavior at high substrate concentrations.[15] We consider whether this is due to substrate inhibition, as previously suggested, or possibly a result of partial denaturation of the protein in the presence of high concentrations of substituted phenols. When 1 mM 2,4,6-TCP was added with urea, the $\Delta G_D(H_2O)$ of DHP A decreased from 6.80 ± 0.85 to 2.81 ± 0.19 kcal/mol. Substrate inhibition of DHP A occurs at ∼2 mM 2,4,6-TCP. Therefore, if increasing the 2,4,6-TCP concentration destabilizes with a linear dependence that is the same as that of 4-BP (shown in Table 1), at 2 mM TCP it would cause $\Delta G_D(H_2O)$ to be ≤0, which means DHP A would be in its unfolded state. Therefore, the decline in the catalytic rate that has been attributed to substrate inhibition may be due to the destabilizing effect of 2,4,6-TXPs on protein stability.[15] Two possible factors that could contribute to the lower catalytic activity are (1) lower protein concentrations due to protein desolvation and/or precipitation with higher concentrations of halophenols and (2) partial unfolding at higher concentrations leading to weaker binding.

Comparison of DSC and titrations of denaturants lead to the conclusion that there are intermediates even in the loss of heme and a two-state model cannot account for all of the data. While titrations of GdnHCl and urea alone appear to show that the loss of heme from DHP A is consistent with a two-state model, DHP B is more complicated and deviates from a two-state model for the urea titration. Both GdnHCl-mediated denaturation and urea-mediated denaturation have a greater

destabilizing effect on DHP B. Furthermore, thermal denaturation via DSC shows DHP B has a lower $T_m$ and $\Delta H$ (bond energy) to maintain the native state. The lower stability of DHP B may be connected to the greater substrate inhibition effect seen in kinetics because increased activity is correlated with greater access of halophenols to the distal pocket and heme itself.

**Effects of Organic Solvents on Stability and Enzymatic Activity.** Phenols are a well-known class of protein denaturants that have been shown to cause a decrease in enzymatic activity. This is often correlated to removal of the water shell, which causes desolvation, protein unfolding, and ultimately denaturation. DHP has a lower tolerance to organic solvent desolvation than other globins. The cold acid–butanone method has been used to successfully prepare apomyoglobin, apohemoglobin, apoHRP, apocytochrome, etc.;[23,32,43,55,56] however, the addition of butanone to DHP results in immediate aggregation and precipitation. This observation is consistent with the lower stability of heme in the globin observed in our study because it probably arises from a larger exposed hydrophobic surface area. While DHP tolerates low concentrations of methanol tested to increase the solubility of hydrophobic substrates such as 2,4,6-TBP, solvents such as 2-isopropanol are quite destabilizing. Moreover, Figure 9 shows that increasing concentrations of MeOH decrease $V_{max}$ and enzymatic activity. We must consider these observations in the context of the known ability of certain enzymes to function in organic solvents.[57] DHP is not like these proteins because it binds strongly hydrophobic phenolic substrates at internal sites. This facet of its enzymatic activity makes interior hydrophobic residues more solvent accessible in DHP than in many other enzymes or globins.

We can make an analogy between the effect of the increased hydrophobicity of the halophenolic substrate, e.g., due to the halogen atom (2,4,6-TBP > 2,4,6-TCP), and the effect of increasingly hydrophobic solvents; both destabilize the heme and thereby also decrease catalytic efficiency. For example, a decrease in catalytic activity in 10% 2-PrOH and 10% MeOH, for DHP by ∼50 and ∼25%, respectively,[15] correlates with an enhancement of the denaturing ability of alcohols due to the increasing hydrocarbon content (PrOH > EtOH > MeOH).[58] Likewise, halophenolic substrates promote expansion of the active site and promote higher rates of hemin loss when exposed to the solvent (Figure 12). The fact that 2,4,6-TBP is a stronger denaturant and larger than 2,4,6-TCP may explain why there is a greater turnover rate for 2,4,6-TCP then for the "native substrate", 2,4,6-TBP. DHP A and DHP B oxidize 2,4,6-TCP 2–3 times better than the native substrate 2,4,6-TBP. Moreover, these observations are consistent with substrate inhibition[15,16] at a concentration of 2,4,6-TBP lower than that of 2,4,6-TCP because 2,4,6-TBP is a stronger denaturant.

**Relationship to Sperm Whale Myoglobin.** The crystal structures and amino acid sequence of DHP indicate that DHP has a common ancestry with the oxygen carrier globin family,[59,60] but mechanistic studies have reached a consensus that DHP has the capability of oxidizing substrate by the same mechanism that is used by horseradish peroxidase (HRP).[17,29,61] The peroxidase activity of DHP is believed to arise mainly through conformational control of the proximal and distal histidine, which result in the increased basicity of the proximal histidine and the increased flexibility of the distal histidine required to facilitate peroxidase function.[9] Despite the structural similarity to sperm whale myoglobin (SWMb),[47,62]

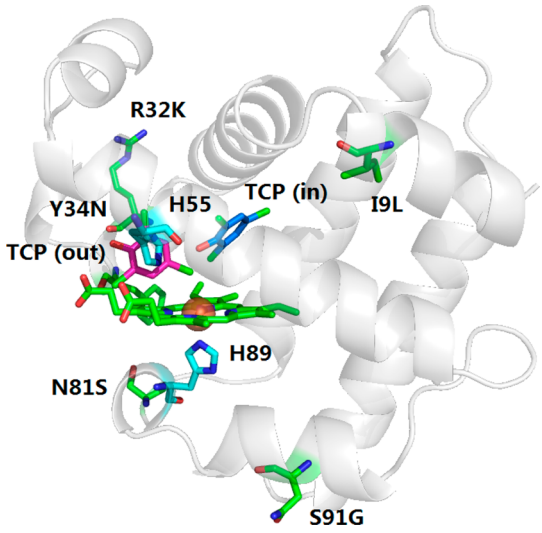


**Figure 12.** Key amino acid mutations that convert DHP A into DHP B with TCP bound at two binding sites. The five amino acid changes required to convert DHP A into DHP B are I9L, R32K, Y34N, N81S, and S91G.

DHP has a lower $T_m$ and a lower Gibbs free energy of unfolding, indicating that it is a less stable protein. Denaturation profiles of SWMb with DSC showed a single endothermic peak at ∼85 °C,[63] while DHP A has an endothermic peak at ∼50.4 °C. Clearly, similar structure does not indicate similar folding stability, and the folding stability is dependent on the sequence of the amino acid, which is significantly different given the low level of sequence homology of 17% between these two proteins.

*A. ornata* is a simple organism that has no liver or other organs that specialize in detoxification. Therefore, we hypothesize that DHP acquired a diverse range of functions (oxygen transporter, peroxidase, peroxygenase, and disulfide oxidase) to facilitate the survival of *A. ornata*. The high flexibility of intrinsically disordered proteins provides many advantages for function, which may be particularly important for multifunctional proteins.[64]

**Reciprocal Relationship of Folding Stability and Catalytic Activity.** The biological function of many proteins is controlled by conformational change where ligand and substrate binding is a dynamic process that demands flexibility.[64] Because the essence of catalysis is stabilization of the transition state,[65] a rigid structure would be active only if it could bind the transition state geometry. While this type of binding does occur to some extent, it is also clear dynamic interactions can facilitate activation by forcing the substrate to move along a reaction coordinate. The compact globular structure of proteins seen in X-ray crystal structures may not capture the dynamic nature of proteins involved in catalysis.[66] Aside from the lower heme binding affinity, DHP's thermal profiles differ from those of SWMb in that they do not follow a two-state model.

The multifunctional nature of DHP may be facilitated by the flexibility indicated by such a model. Previous studies of DHP suggest that an inhibitor for one chemical reaction may share the same local domain and/or region as a substrate for another chemical reaction catalyzed by DHP. For example, it may be that the binding of 2,4,6-TBP to the internal site does not facilitate peroxidase chemistry. That site may be active for only peroxygenase chemistry.[6] Additionally, the inhibitor-binding


dx.doi.org/10.1021/bi5005975 | *Biochemistry* 2014, 53, 6863–6877

site for *p*-halophenols (4-XP) may be a substrate-binding site for hydroquinone ($H_2Q$).[67] Myoglobins (e.g., SWMb, HSMb, and HHMb) function to sequester bound $O_2$, which is facilitated by a high degree of hydrophobicity in the distal pocket. Myoglobins are consequently poor peroxidases.[68−70]

Residues that participate in catalysis or ligand or substrate binding are not necessarily optimized to maximize the binding affinity of the heme or the stability of the surrounding globin. Therefore, it may be possible to substitute these crucial residues to produce a more stable protein at the expense of catalytic activity. On the basis of previous mutational studies involving the heme active site and distal histidine of DHP,[71−73] we consider how point mutations involving the distal, internal inhibitor-binding site and the surrounding residues can lead to a stability−function trade-off. We emphasize that the hypothesis of an inverse correlation between heme binding affinity and peroxidase activity is based primarily on the observation that the flexibility of the distal histidine[74,75] is responsible for the increased rate of peroxidase activity relative to other globins. The distal pocket of DHP is larger, as well, which means that despite its high degree of hydrophobicity it is more malleable that then distal pocket of other myoglobins and hemoglobins. The reason for this increase is that $H_2O_2$ must enter the distal pocket and replace $O_2$,[2] which in turn can explain how a ferrous heme[76] can conduct peroxidase chemistry.[7] As a relevant example, the distal histidine in heme proteins is required for hydrogen bonding interactions with oxygen, inhibition of autoxidation, and discrimination against CO binding.[77] Previous studies of SWMb showed that the functionality of the distal histidine decreased with increased stability. Aliphatic or aromatic substitutions for the distal histidine (at position H64 in apoSWMb) produce apoglobins that are more stable than wild-type apoprotein.[24] Replacing the polar distal His with a hydrophobic Leu or Phe stabilizes the apoprotein 20−30-fold, and the H64A mutation stabilized the apoprotein 6-fold with respect to wild-type apoprotein. The increase in stability is most likely attributed to removing a polar residue from the hydrophobic core and therefore improving hydrophobic and van der Waals interactions. Increasing the hydrophobicity of the heme pocket[44] increases the binding affinity of the heme and stabilizes a five-coordinate mono-histidine adduct, but it is not desirable for peroxidase function. Because the peroxidase function requires protein fluctuations to permit two molecules ($H_2O_2$ and $O_2$) simultaneously in the distal pocket,[78] the very increase in hydrophobicity that increases heme binding affinity also would be expected to decrease the access of those molecules to the distal pocket as required for peroxidase function.[8,79]

The distal histidine in DHP (H55) is required for both oxygen transport and peroxidase function in DHP. Because DHP has no hydrogen bonding amino acids in the distal pocket, other than the distal histidine, it is clear that this amino acid must play a role in acid−base catalysis that may accommodate more than one oxidative mechanism. This distinguishes DHP from peroxidases, which have at least one other polar amino acid (e.g., arginine) in the distal pocket that aids in the activation of $H_2O_2$ bound to the heme Fe.[80] For this reason, we have postulated that the flexibility of the distal histidine is a unique feature required for DHP function.[75,76,81] H55 acts as an acid base catalyst to form a ferryl intermediate for the activation of peroxidase function.[30] As observed in SWMb, mutations at this position can greatly affect the enzymatic activity. Substituting the distal histidine for valine (H55V), an aliphatic residue, showed no peroxidase activity because it would leave no residue for protonation of the ferryl intermediate.[79,82] In our study, the H55V mutant exhibited a greater resistance to chemical and thermal denaturation and a rate of heme dissociation lower than that of DHP A. The replacement of a polar histidine with a nonpolar valine results in stabilization of the hydrophobic core. The consequence is greater binding affinity of the heme and greater protein stability, but a complete loss of peroxidase activity. In SWMb, a similar mutation, H64V, results in destabilization of the heme.[25] This effect in SWMb is attributed to the destabilization of the heme-bound $H_2O$ molecule. In DHP A, the $H_2O$ molecule is already largely destabilized; i.e., the distal pocket is more hydrophobic than in SWMb. However, the distal valine in DHP A leads to a reduction in the openness of the distal pocket, which stabilizes the heme.

**Relationship between DHP A and B.** We are interested in how the five-amino acid difference in DHP B causes it to be less stable yet more catalytically active than DHP A. Does DHP B gain its increase in catalytic efficiency at the expense of folding stability? The five-amino acid difference is conservative in that it is charge neutral and results in an only modest change in polarity (Figure 1). The mutations are mostly on the surface. The effect of the mutations appears to be mostly a shift in the structure of the hydrophobic core produced by altering the packing of the interior amino acid side chains. None of the amino acids that separate DHP A from B directly affect the binding of the substrate or cosubstrate, but they do affect enzyme kinetics and folding stability. We hypothesize that the effect on function is indirect and results from the increased flexibility in a general sense. When DHP B is compared to DHP A, the substitutions of asparagine for tyrosine (Y34N) and glycine for serine (S91G) both decrease the helical propensity and therefore potentially reduce the stability of the $\alpha$-helical structure. Peroxidase function depends on both the distal hydrogen bonding interactions with bound $H_2O_2$ and the strength of proximal ligation to the heme Fe.[73] Recent evidence suggests that I9L has the largest effect on rate of all of the mutants. This is an unusual observation because this is a minor change and is quite far from the heme. The most likely reason for the change is that the packing of hydrophobic amino acids (F60, F21, and L100) may be affected and that this may affect substrate binding. Once again, the same effect that permits dynamic motions and entry of the substrate may result in a decrease in folding stability.

Because none of the five amino acids that are different in DHP A and B directly participate in catalytic function, we hypothesize that the main effect is a general increase in dynamic motion linked to uptake of the substrate and possibly the cosubstrate, $H_2O_2$. In other systems, NMR evidence suggests that a highly dynamic, non-native conformation is compatible with efficient catalysis.[83] One can view the dynamic nature of an enzyme active site as a partially unfolded state of a protein. In this view, complexes between the molten globule state/partial fold and the ligand retain considerable conformational plasticity, which permits efficient catalysis.[83,84]

## ■ CONCLUSION

Understanding the interaction of inhibitors and substrates with DHP must take include the threshold above which DHP begins to lose its heme and unfold. Phenols can act as substrates or inhibitors but are also themselves denaturants, which accelerate the rate of heme loss causing protein desolvation and


dx.doi.org/10.1021/bi5005975 | *Biochemistry* 2014, 53, 6863−6877

precipitation. DHP shows an inverse relationship between heme affinity and enzymatic activity, where the ligation of $H_2O$, flexibility of the distal histidine, and hydrophobic residue stabilization are three key factors. A more rigid and/or stable structure restricts heme access to requisite molecules ($O_2$ exiting and $H_2O_2$ entering), which is needed for activation of bound $H_2O_2$. Therefore, greater dynamic motion (arising from protein instability) can result in greater enzymatic activity (i.e., DHP A and DHP B).

## ■ ASSOCIATED CONTENT

### Supporting Information

An analysis of the fitting method applied to DSC data. This material is available free of charge via the Internet at http://pubs.acs.org.

## ■ AUTHOR INFORMATION


### Corresponding Author

*Phone: 919-515-8915. Fax: 919-515-8920. E-mail: stefan_franzen@ncsu.edu.



### Funding

This project was supported by Army Research Office Grant 57861-LS.


### Notes

The authors declare no competing financial interest.

## ■ ABBREVIATIONS

2,6-DBQ, 2,6-dibromoquinone; 2,6-DCQ, 2,6-dichloroquinone; DHP A, dehaloperoxidase-hemoglobin A; DHP B, dehaloperoxidase-hemoglobin B; HSMb, horse skeletal muscle myoglobin; HHMb, horse heart myoglobin; SWMb, sperm whale myoglobin; 2,4,6-TBP, 2,4,6-tribromophenol; 2,4,6-TCP, 2,4,6-trichlorophenol; 2-PrOH, 2-propanol; MeOH, methanol; GdnHCl, guanidinium hydrochloride; DMSO, dimethyl sulfoxide; NMR, nuclear magnetic resonance; DSC, differential scanning calorimetry.

## ■ REFERENCES


(1) Chen, Y. P., Woodin, S. A., Lincoln, D. E., and Lovell, C. R. (1996) An unusual dehalogenating peroxidase from the marine terebellid polychaete *Amphitrite ornata*. *J. Biol. Chem. 271*, 4609−4612.

(2) D'Antonio, J., and Ghiladi, R. A. (2011) Reactivity of Deoxy- and Oxyferrous Dehaloperoxidase B from *Amphitrite ornata*: Identification of Compound II and Its Ferrous-Hydroperoxide Precursor. *Biochemistry 50*, 5999−6011.

(3) Han, K., Woodin, S. A., Lincoln, D. E., Fielman, K. T., and Ely, B. (2001) *Amphitrite ornata*, a marine worm, contains two dehaloperoxidase genes. *Mar. Biotechnol. 3*, 287−292.

(4) Weber, R. E., Mangum, C., Steinman, H., Bonaventura, C., Sullivan, B., and Bonaventura, J. (1977) Hemoglobins of two terebellid polychaetes: *Enoplobranchus sanguineus* and *Amphitrite ornata*. *Comp. Biochem. Physiol., Part A: Mol. Integr. Physiol. 56*, 179−187.

(5) Nicoletti, F. P., Thompson, M. K., Franzen, S., and Smulevich, G. (2011) Degradation of sulfide by dehaloperoxidase-hemoglobin from *Amphitrite ornata*. *JBIC, J. Biol. Inorg. Chem. 16*, 611−619.

(6) Barrios, D., D'Antonio, J., McCombs, N., Zhao, J., Franzen, S., Schmidt, A. C., Sombers, L. A., and Ghiladi, R. A. (2014) Peroxygenase and Oxidase Activities of Dehaloperoxidase-Hemoglobin from *Amphitrite ornata*. *J. Am. Chem. Soc. 136*, 7914−7925.

(7) Franzen, S., Thompson, M. K., and Ghiladi, R. A. (2012) The dehaloperoxidase paradox. *Biochem. Biophys. Acta 1824*, 578−588.

(8) Du, J., Sono, M., and Dawson, J. H. (2010) Functional Switching of *Amphitrite ornata* Dehaloperoxidase from $O_2$-Binding Globin to Peroxidase Enzyme Facilitated by Halophenol Substrate and $H_2O_2$. *Biochemistry 49*, 6064−6069.

(9) LaCount, M. W., Zhang, E., Chen, Y. P., Han, K., Whitton, M. M., Lincoln, D. E., Woodin, S. A., and Lebioda, L. (2000) The crystal structure and amino acid sequence of dehaloperoxidase from *Amphitrite ornata* indicate common ancestry with globins. *J. Biol. Chem. 275*, 18712−18716.

(10) Lebioda, L., LaCount, M. W., Zhang, E. L., Chen, Y. P., Han, K. P., Whitton, M. M., Lincoln, D. E., and Woodin, S. A. (1999) Protein structure: An enzymatic globin from a marine worm. *Nature 401*, 445.

(11) Nicoletti, F. P., Thompson, M. K., Howes, B. D., Franzen, S., and Smulevich, G. (2010) New insights into the role of distal histidine flexibility in ligand stabilization of dehaloperoxidase-hemoglobin from *Amphitrite ornata*. *Biochemistry 49*, 1903−1912.

(12) Thompson, M. K., Davis, M. F., de Serrano, V., Nicoletti, F. P., Howes, B. D., Smulevich, G., and Franzen, S. (2010) Internal binding of halogenated phenols in dehaloperoxidase-hemoglobin inhibits peroxidase function. *Biophys. J. 99*, 1586−1595.

(13) Davis, M. F., Bobay, B. G., and Franzen, S. (2010) Determination of Separate Inhibitor and Substrate Binding Sites in the Dehaloperoxidase-Hemoglobin from *Amphitrite ornata*. *Biochemistry 49*, 1199−1206.

(14) Davis, M. F., Gracz, H., Vendeix, F. A. P., de Serrano, V., Somasundaram, A., Decatur, S. M., and Franzen, S. (2009) Different Modes of Binding of Mono-, Di-, and Trihalogenated Phenols to the Hemoglobin Dehaloperoxidase from *Amphitrite ornata*. *Biochemistry 48*, 2164−2172.

(15) Zhao, J., de Serrano, V., Zhao, J. J., Le, P., and Franzen, S. (2013) Structural and Kinetic Study of an Internal Substrate Binding Site in Dehaloperoxidase-Hemoglobin A from *Amphitrite ornata*. *Biochemistry 52*, 2427−2439.

(16) Wang, C., Lovelace, L. L., Sun, S., Dawson, J. H., and Lebioda, L. (2013) Complexes of Dual-Function Hemoglobin/Dehaloperoxidase with Substrate 2,4,6-Trichlorophenol Are Inhibitory and Indicate Binding of Halophenol to Compound I. *Biochemistry 52*, 6203−6210.

(17) Sturgeon, B. E., Battenburg, B. J., Lyon, B. J., and Franzen, S. (2011) Revisiting the peroxidase oxidation of 2,4,6-trihalophenols: ESR detection of radical intermediates. *Chem. Res. Toxicol. 24*, 1862−1868.

(18) Schkolnik, G., Utesch, T., Zhao, J. J., Jiang, S., Thompson, M. K., Mroginski, M. A., Hildebrandt, P., and Franzen, S. (2013) Catalytic efficiency of dehaloperoxidase A is controlled by electrostatics: Application of the vibrational Stark effect to understand enzyme kinetics. *Biochem. Biophys. Res. Commun. 430*, 1011−1015.

(19) Franzen, S., Sasan, K., Sturgeon, B. E., Lyon, B. J., Battenburg, B. J., Gracz, H., Dumariah, R., and Ghiladi, R. (2012) Nonphotochemical Base-Catalyzed Hydroxylation of 2,6-Dichloroquinone by $H_2O_2$ Occurs by a Radical Mechanism. *J. Phys. Chem. B 116*, 1666−1676.

(20) Ator, M. A., and Ortiz de Montellano, P. R. (1987) Protein control of prosthetic heme reactivity. Reaction of substrates with the heme edge of horseradish peroxidase. *J. Biol. Chem. 262*, 1542−1551.

(21) Freire, E., and Xie, D. (1994) Thermodynamic prediction of structural determinants of the molten globule state of barnase. *Biophys. Chem. 51*, 243−251.

(22) Luque, I., and Freire, E. (2000) Structural stability of binding sites: Consequences for binding affinity and allosteric effects. *Proteins Suppl. 4*, 63−71.

(23) Hargrove, M. S., and Olson, J. S. (1996) The stability of holomyoglobin is determined by heme affinity. *Biochemistry 35*, 11310−11318.

(24) Hargrove, M. S., Krzywda, S., Wilkinson, A. J., Dou, Y., Ikeda-Saito, M., and Olson, J. S. (1994) Stability of myoglobin: A model for the folding of heme proteins. *Biochemistry 33*, 11767−11775.

(25) Hargrove, M. S., Wilkinson, A. J., and Olson, J. S. (1996) Structural factors governing hemin dissociation from metmyoglobin. *Biochemistry 35*, 11300−11309.

(26) de Serrano, V., D'Antonio, J., Franzen, S., and Ghiladi, R. A. (2010) Structure of dehaloperoxidase B at 1.58 angstrom resolution

and structural characterization of the AB dimer from *Amphitrite ornata*. *Acta Crystallogr. D66*, 529−538.
(27) D'Antonio, J., D'Antonio, E. L., Thompson, M. K., Bowden, E. F., Franzen, S., Smirnova, T., and Ghiladi, R. A. (2010) Spectroscopic and Mechanistic Investigations of Dehaloperoxidase B from *Amphitrite ornata*. *Biochemistry 49*, 6600−6616.
(28) de Serrano, V., and Franzen, S. (2012) Structural evidence for stabilization of inhibitor binding by a protein cavity in the dehaloperoxidase-hemoglobin from *Amphitrite ornata*. *Pept. Sci. 98*, 27−35.
(29) Ma, H., Thompson, M. K., Gaff, J., and Franzen, S. (2010) Kinetic analysis of a naturally occurring bioremediation enzyme: Dehaloperoxidase-hemoglobin from *Amphitrite ornata*. *J. Phys. Chem. B 114*, 13823−13829.
(30) Zhao, J., de Serrano, V., Dumarieh, R., Thompson, M., Ghiladi, R. A., and Franzen, S. (2012) The role of the distal histidine in $H_2O_2$ activation and heme protection in both peroxidase and globin functions. *J. Phys. Chem. B 116*, 12065−12077.
(31) Teale, F. W. J. (1959) Cleavage of the Haem-Protein Link by Acid Methylethylketone. *Biochim. Biophys. Acta 35*, 543.
(32) Ascoli, F., Fanelli, M. R., and Antonini, E. (1981) Preparation and properties of apohemoglobin and reconstituted hemoglobins. *Methods Enzymol. 76*, 72−87.
(33) Gattoni, M., Boffi, A., and Chiancone, E. (1998) Immobilized apo-myoglobin, a new stable reagent for measuring rates of heme dissociation from hemoglobin. *FEBS Lett. 424*, 275−278.
(34) Jones, C. M. (1997) An Introduction to Research in Protein Folding for Undergraduates. *J. Chem. Educ. 74*, 1306.
(35) Sykes, P. A., Shiue, H.-C., Walker, J. R., and Bateman, R. C. (1999) Determination of Myoglobin Stability by Visible Spectroscopy. *J. Chem. Educ. 76*, 1283.
(36) Watlaufer, D. B., Malik, S. K., Stoller, L., and Coffin, R. L. (1964) Nonpolar Group Participation in the Denaturation of Proteins by Urea and Guanidinium Salts. Model Compound Studies. *J. Am. Chem. Soc. 86*, 508−514.
(37) Almarza, J., Rincon, L., Bahsas, A., and Brito, F. (2009) Molecular mechanism for the denaturation of proteins by urea. *Biochemistry 48*, 7608−7613.
(38) Bennion, B. J., and Daggett, V. (2003) The molecular basis for the chemical denaturation of proteins by urea. *Proc. Natl. Acad. Sci. U.S.A. 100*, 5142−5147.
(39) Plummer, A., Thompson, M. K., and Franzen, S. (2013) Role of Polarity of the Distal Pocket in the Control of Inhibitor Binding in Dehaloperoxidase-Hemoglobin. *Biochemistry 52*, 2218−2227.
(40) Sutherland, J. W. (1977) Disagreement between calorimetric and van't Hoff enthalpies of assembly of protein supramolecular structures. *Proc. Natl. Acad. Sci. U.S.A. 74*, 2002−2006.
(41) Kresheck, G. C., and Erman, J. E. (1988) Calorimetric studies of the thermal denaturation of cytochrome c peroxidase. *Biochemistry 27*, 2490−2496.
(42) Hargrove, M. S., Singleton, E. W., Quillin, M. L., Ortiz, L. A., Phillips, G. N., Jr., Olson, J. S., and Mathews, A. J. (1994) His64(E7)→Tyr apomyoglobin as a reagent for measuring rates of hemin dissociation. *J. Biol. Chem. 269*, 4207−4214.
(43) Fioretti, E., Ascoli, F., and Brunori, M. (1976) Preparation of apohemoglobin trout IV and reconstitution with different hemes. *Biochem. Biophys. Res. Commun. 68*, 1169−1173.
(44) Liong, E. C., Dou, Y., Scott, E. E., Olson, J. S., and Phillips, G. N., Jr. (2000) Waterproofing the heme pocket. *J. Biol. Chem. 276*, 9093−9100.
(45) Smith, M. L., Paul, J., Ohlsson, P. I., Hjortsberg, K., and Paul, K. G. (1991) Heme-protein fission under nondenaturing conditions. *Proc. Natl. Acad. Sci. U.S.A. 88*, 882−886.
(46) Feducia, J., Dumarieh, R., Gilvey, L. B. G., Smirnova, T., Franzen, S., and Ghiladi, R. A. (2009) Characterization of Dehaloperoxidase Compound ES and Its Reactivity with Trihalophenols. *Biochemistry 48*, 995−1005.
(47) de Serrano, V., Chen, Z. X., Davis, M. F., and Franzen, S. (2007) X-ray crystal structural analysis of the binding site in the ferric and oxyferrous forms of the recombinant heme dehaloperoxidase cloned from *Amphitrite ornata*. *Acta Crystallogr. D63*, 1094−1101.
(48) Zhao, J., and Franzen, S. (2013) Kinetic Study of the Inhibition Mechanism of Dehaloperoxidase-Hemoglobin A by 4-Bromophenol. *J. Phys. Chem. B 117*, 8301−8309.
(49) Parsons, G. H., Rochester, C. H., and Wood, C. E. C. (1971) Effect of 4-substitution on the thermodynamics of hydration of phenol and the phenoxide anion. *J. Chem. Soc. B*, 533−536.
(50) Pace, C. N. (1975) The stability of globular proteins. *CRC Crit. Rev. Biochem. 3*, 1−43.
(51) Deshpande, R. A., Khan, M. I., and Shankar, V. (2003) Equilibrium unfolding of RNase Rs from *Rhizopus stolonifer*: pH dependence of chemical and thermal denaturation. *Biochim. Biophys. Acta 1648*, 184−194.
(52) Park, Y. D., Jung, J. Y., Kim, D. W., Kim, W. S., Hahn, M. J., and Yang, J. M. (2003) Kinetic inactivation study of mushroom tyrosinase: Intermediate detection by denaturants. *J. Protein Chem. 22*, 463−471.
(53) Inouye, K., Tanaka, H., and Oneda, H. (2000) States of tryptophyl residues and stability of recombinant human matrix metalloproteinase 7 (matrilysin) as examined by fluorescence. *J. Biochem. 128*, 363−369.
(54) Yao, M., and Bolen, D. W. (1995) How valid are denaturant-induced unfolding free energy measurements? Level of conformance to common assumptions over an extended range of ribonuclease A stability. *Biochemistry 34*, 3771−3781.
(55) Lasagna, M., Gratton, E., Jameson, D. M., and Brunet, J. E. (1999) Apohorseradish peroxidase unfolding and refolding: Intrinsic tryptophan fluorescence studies. *Biophys. J. 76*, 443−450.
(56) Tomlinson, E. J., and Ferguson, S. J. (2000) Conversion of a c type cytochrome to a b type that spontaneously forms in vitro from apo protein and heme: Implications for c type cytochrome biogenesis and folding. *Proc. Natl. Acad. Sci. U.S.A. 97*, 5156−5160.
(57) Klibanov, A. M. (2001) Improving enzymes by using them in organic solvents. *Nature 409*, 241−246.
(58) Figueiredo, K. C., Ferraz, H. C., Borges, C. P., and Alves, T. L. (2009) Structural stability of myoglobin in organic media. *Protein J. 28*, 224−232.
(59) Bailly, X., Chabasse, C., Hourdez, S., Dewilde, S., Martial, S., Moens, L., and Zal, F. (2007) Globin gene family evolution and functional diversification in annelids. *FEBS J. 274*, 2641−2652.
(60) Hardison, R. (1998) Hemoglobins from bacteria to man: Evolution of different patterns of gene expression. *J. Exp. Biol. 201*, 1099−1117.
(61) Osborne, R. L., Coggins, M. K., Raner, G. M., Walla, M., and Dawson, J. H. (2009) The mechanism of oxidative halophenol dehalogenation by *Amphitrite ornata* dehaloperoxidase is initiated by $H_2O_2$ binding and involves two consecutive one-electron steps: Role of ferryl intermediates. *Biochemistry 48*, 4231−4238.
(62) Zhang, E., Chen, Y. P., Roach, M. P., Lincoln, D. E., Lovell, C. R., Woodin, S. A., Dawson, J. H., and Lebioda, L. (1996) Crystallization and initial spectroscopic characterization of the heme-containing dehaloperoxidase from the marine polychaete *Amphitrite ornata*. *Acta Crystallogr. DS2*, 1191−1193.
(63) Regis, W. C., Fattori, J., Santoro, M. M., Jamin, M., and Ramos, C. H. (2005) On the difference in stability between horse and sperm whale myoglobins. *Arch. Biochem. Biophys. 436*, 168−177.
(64) Smith, A. J. T., Muller, R., Toscano, M. D., Kast, P., Hellinga, H. W., Hilvert, D., and Houk, K. N. (2008) Structural Reorganization and Preorganization in Enzyme Active Sites: Comparisons of Experimental and Theoretically Ideal Active Site Geometries in the Multistep Serine Esterase Reaction Cycle. *J. Am. Chem. Soc. 130*, 15361−15373.
(65) Wolfenden, R. (2011) Benchmark Reaction Rates, the Stability of Biological Molecules in Water, and the Evolution of Catalytic Power in Enzymes. In *Annual Reviews of Biochemistry* (Kornberg, R. D., Raetz, C. R. H., Rothman, J. E., and Thorner, J. W., Eds.) pp 645−667, Annual Reviews, Palo Alto, CA.
(66) Schulenburg, C., and Hilvert, D. (2013) Protein Conformational Disorder and Enzyme Catalysis. In *Dynamics in Enzyme Catalysis*

(Klinman, J., and Hammes-Schiffer, S., Eds.) pp 41−67, Springer, Berlin.
(67) Zhao, J., Zhao, J., and Franzen, S. (2013) The regulatory implications of hydroquinone for the multifunctional enzyme dehaloperoxidase-hemoglobin from *Amphitrite ornata*. *J. Phys. Chem. B 117*, 14615−14624.
(68) George, P., and Irvine, D. H. (1952) The reaction of metmyoglobin with hydrogen peroxide. *Biochem. J. 52*, 511−517.
(69) George, P., and Irvine, D. H. (1953) The Higher Oxidation State of Metmyoglobin. *Biochem. J. 53*, R25.
(70) Osborne, R. L., Coggins, M. K., Walla, M., and Dawson, J. H. (2007) Horse Heart Myoglobin Catalyzes the $H_2O_2$-Dependent Oxidative Dehalogenation of Chlorophenols to DNA-Binding Radicals and Quinones. *Biochemistry 46*, 9823−9829.
(71) Franzen, S., Belyea, J., Gilvey, L. B., Davis, M. F., Chaudhary, C. E., Sit, T. L., and Lommel, S. A. (2006) Proximal cavity, distal histidine, and substrate hydrogen-bonding mutations modulate the activity of *Amphitrite ornata* dehaloperoxidase. *Biochemistry 45*, 9085−9094.
(72) Du, J., Huang, X., Sun, S. F., Wang, C. X., Lebioda, L., and Dawson, J. H. (2011) *Amphitrite ornata* Dehaloperoxidase (DHP): Investigations of Structural Factors That Influence the Mechanism of Halophenol Dehalogenation Using "Peroxidase-like" Myoglobin Mutants and "Myoglobin-like" DHP Mutants. *Biochemistry 50*, 8172−8180.
(73) Jiang, S., Wright, I., Swartz, P., and Franzen, S. (2013) The role of T56 in controlling the flexibility of the distal histidine in dehaloperoxidase-hemoglobin from *Amphitrite ornata*. *Biochim. Biophys. Acta 1834*, 2020−2029.
(74) Zhao, J., de Serrano, V., and Franzen, S. (2014) A Model for the Flexibility of the Distal Histidine in Dehaloperoxidase-Hemoglobin A Based on X-ray Crystal Structures of the Carbon Monoxide Adduct. *Biochemistry 53*, 2474−2479.
(75) Chen, Z., De Serrano, V., Betts, L., and Franzen, S. (2009) Distal histidine conformational flexibility in dehaloperoxidase from *Amphitrite ornata*. *Acta Crystallogr. D65*, 34−40.
(76) D'Antonio, E. L., Bowden, E. F., and Franzen, S. (2012) Thin-layer spectroelectrochemistry of the Fe(III)/Fe(II) redox reaction of dehaloperoxidase-hemoglobin. *J. Electroanal. Chem. 668*, 37−43.
(77) Brantley, R. E., Jr., Smerdon, S. J., Wilkinson, A. J., Singleton, E. W., and Olson, J. S. (1993) The mechanism of autooxidation of myoglobin. *J. Biol. Chem. 268*, 6995−7010.
(78) Zhao, J., Srajer, V., and Franzen, S. (2013) Functional consequences of the open distal pocket of dehaloperoxidase-hemoglobin observed by time-resolved X-ray crystallography. *Biochemistry 52*, 7943−7950.
(79) Davydov, R., Osborne, R. L., Shanmugam, M., Du, J., Dawson, J. H., and Hoffman, B. M. (2010) Probing the oxyferrous and catalytically active ferryl states of *Amphitrite ornata* dehaloperoxidase by cryoreduction and EPR/ENDOR spectroscopy. Detection of compound I. *J. Am. Chem. Soc. 132*, 14995−15004.
(80) Gajhede, M., Schuller, D. J., Henriksen, A., Smith, A. T., and Poulos, T. L. (1997) Crystal structure of horseradish peroxidase C at 2.15 angstrom resolution. *Nat. Struct. Biol. 4*, 1032−1038.
(81) de Serrano, V. S., Davis, M. F., Gaff, J. F., Zhang, Q., Chen, Z., D'Antonio, E. L., Bowden, E. F., Rose, R., and Franzen, S. (2010) X-ray structure of the metcyano form of dehaloperoxidase from *Amphitrite ornata*: Evidence for photoreductive dissociation of the iron-cyanide bond. *Acta Crystallogr. D66*, 770−782.
(82) Davydov, R., Osborne, R. L., Kim, S. H., Dawson, J. H., and Hoffman, B. M. (2008) EPR and ENDOR studies of cryoreduced compounds II of peroxidases and myoglobin. Proton-coupled electron transfer and protonation status of ferryl hemes. *Biochemistry 47*, 5147−5155.
(83) Pervushin, K., Vamvaca, K., Vogeli, B., and Hilvert, D. (2007) Structure and dynamics of a molten globular enzyme. *Nat. Struct. Mol. Biol. 14*, 1202−1206.
(84) Bemporad, F., Gsponer, J., Hopearuoho, H. I., Plakoutsi, G., Stati, G., Stefani, M., Taddei, N., Vendruscolo, M., and Chiti, F. (2008) Biological function in a non-native partially folded state of a protein. *EMBO J. 27*, 1525−1535.